

## Enhanced Bioavailability of a Poorly Soluble VR1 Antagonist Using an Amorphous Solid Dispersion Approach: A Case Study

Michael Kennedy,<sup>\*,†</sup> Jack Hu,<sup>†</sup> Ping Gao,<sup>†</sup> Lan Li,<sup>†</sup> Alana Ali-Reynolds,<sup>†</sup> Ben Chal,<sup>†</sup> Vicki Gupta,<sup>†</sup> Chandra Ma,<sup>†</sup> Nidhi Mahajan,<sup>†</sup> Anna Akrami,<sup>‡</sup> and Sekhar Surapaneni<sup>‡</sup>

*Small Molecule Process & Product Development, Amgen Inc., Thousand Oaks, California 91320, and Pharmacokinetics and Drug Metabolism, Amgen Inc., Thousand Oaks, California 91320*

Received June 6, 2008; Revised Manuscript Received September 22, 2008; Accepted October 16, 2008

**Abstract:** Amorphous solid dispersions (ASD) of a poorly soluble water-soluble VR1 antagonist (AMG 517) were explored for improving physical stability and in vivo exposure. AMG 517 was incorporated at 15 or 50 wt % into polymeric microparticles of hydroxypropyl methylcellulose acetate succinate (HPMCAS) and hydroxypropyl methylcellulose (HPMC) by spray-drying. Solid particles having a collapsed, corrugated structure were observed by SEM. Median particle size ranged from 29 to 40  $\mu\text{m}$  by laser light scattering, and residual solvent levels were below 2% by thermal gravimetric analysis. ASD powders exhibited single glass transition temperatures ( $T_g$ ) in the range of 98–117  $^{\circ}\text{C}$  by modulated DSC and were amorphous by XRPD. Amorphous stability, characterized at 40  $^{\circ}\text{C}$ /75% RH (open dish) by XRPD, was at least six months for ASD formulations. Drug dissolution and supersaturation testing in a USP-2 apparatus indicated superior performance of ASD formulations over micronized AMG 517. PK of an ASD formulation in capsule (15 wt % AMG 517 in HPMCAS blended with 5 wt % SDS) in cynomolgus monkeys ( $n = 6$ , crossover) increased AUC 163% and  $C_{\text{max}}$  145% in comparison to an OraPlus suspension control. The study demonstrates the ASD approach provides improved amorphous physical stability and oral bioavailability for a poorly soluble development-stage molecule.

**Keywords:** Solid dispersion; amorphous stability; HPMC-AS; spray-drying; improved bioavailability

### Introduction

Development of potentially efficacious drug compounds can be hindered by a compound's poor solubility and, as a result, its poor oral bioavailability. Solid dispersion technology is applicable to structurally diverse, poorly water soluble compounds with a wide range of physicochemical properties, and offers the potential of improved bioavailability for these compounds via improved dissolution behavior. Dissolution

and solubility enhancement may be achieved by dispersing the poorly soluble drug in a solid matrix carrier, either as a eutectic or phase separated mixture, or as an amorphous solid dispersion (ASD). The matrix carrier may be a hydrophilic polymer, such as polyvinylpyrrolidone (PVP),<sup>1–7</sup> polyeth-

\* Address correspondence to this author at Amgen Inc. MS 8-2-D, Thousand Oaks, CA 91320. Tel: 805-447-0749. Fax: 805-498-8674. E-mail: kennedy@amgen.com.

<sup>†</sup> Small Molecule Process & Product Development.

<sup>‡</sup> Pharmacokinetics and Drug Metabolism.

- (1) Ambike, A. A.; Mahadik, K. R.; Paradkar, A. Stability study of amorphous valdecoxib. *Int. J. Pharm.* **2004**, 282 (1–2), 151–162.
- (2) Ambike, A. A.; Mahadik, K. R.; Paradkar, A. Spray-dried amorphous solid dispersions of simvastatin, a low T-g drug: In vitro and in vivo evaluations. *Pharm. Res.* **2005**, 22 (6), 990–998.
- (3) Corrigan, O. I.; Holohan, E. M. Amorphous Spray Dried Hydro Flumethiazide Poly Vinyl Pyrrolidone Systems Physicochemical Properties. *J. Pharm. Pharmacol.* **1984**, 36 (4), 217–221.

ylene glycol (PEG),<sup>8,9</sup> or the various cellulose derivatives with broad NF acceptance.<sup>10–25</sup> Application of solid dispersions to improve oral bioavailability of poorly soluble molecules dates back over 40 years, and has been the basis

of several review articles.<sup>26–29</sup> Ideally in an amorphous solid dispersion, the drug is molecularly dispersed within the matrix carrier. Thus, upon exposure to aqueous media, dissolution is believed to generate a supersaturated state due to enhanced dissolution rate of the amorphous, molecularly dispersed drug. The matrix polymer is also believed to have a role in trapping of the drug in a metastable form to prevent precipitation or crystallization from the supersaturated state, either through formation of drug–polymer assemblies or by preventing or retarding nucleation and crystal growth.<sup>29,30</sup>

Over the past two decades, the use of amorphous drugs in solid dispersions has been investigated with practical consideration of product development within the pharmaceutical industry.<sup>27–29,31,32</sup> The primary challenges in developing amorphous drug based solid dispersion formulations relate to assuring long-term physical stability of the drug in the amorphous state, as well as the methods for preparing the formulation on a large scale. In solid dispersions, the matrix material provides benefit in meeting both challenges. Matrix polymers can enhance the storage stability of the solid dispersion by acting as an antiplasticizer, so long as the glass transition temperature ( $T_g$ ) of the polymer is equal to or

- (4) Corrigan, O. I.; Holohan, E. M.; Sabra, K. Amorphous forms of thiazide diuretics prepared by spray-drying. *Int. J. Pharm.* **1984**, *18* (1–2), 195–200.
- (5) Corrigan, O. I.; Sabra, K.; Holohan, E. M. Physicochemical properties of spray dried drugs: Phenobarbitone and hydroflumethiazide. *Drug Dev. Ind. Pharm.* **1983**, *9* (1–2), 1–20.
- (6) Simonelli, A. P.; Mehta, S. C.; Higuchi, W. I. Dissolution rates of high energy polyvinylpyrrolidone (PVP)-sulfathiazole coprecipitates. *J. Pharm. Sci.* **1969**, *58* (5), 538–49.
- (7) Van den Mooter, G.; Wuyts, M.; Bleton, N.; Busson, R.; Grobet, P.; Augustijns, P.; Kinget, R. Physical stabilisation of amorphous ketoconazole in solid dispersions with polyvinylpyrrolidone K25. *Eur. J. Pharm. Sci.* **2001**, *12* (3), 261–269.
- (8) Hajratwala, B. R.; Ho, D. S. Effect of aging on hydrocortisone-polyethylene glycol 4000 and hydrocortisone-polyvinylpyrrolidone dispersions. *J. Pharm. Sci.* **1984**, *73* (11), 1539–41.
- (9) Jachowicz, R.; Nuernberg, E.; Hoppe, R. Solid dispersions of oxazepam. *Int. J. Pharm.* **1993**, *99* (2–3), 321–325.
- (10) Giunchedi, P.; Conte, U.; Maggi, L.; La Manna, A. Hydrophilic matrices for the extended release of a model drug exhibiting pH-dependent solubility. *Int. J. Pharm.* **1992**, *85* (1–3), 141–147.
- (11) Giunchedi, P.; Torre, M. L.; Maggi, L.; Conti, B.; Conte, U. Cellulose acetate trimellitate microspheres containing NSAIDs. *Drug Dev. Ind. Pharm.* **1995**, *21* (3), 315–330.
- (12) Giunchedi, P.; Torre, M. L.; Maggi, L.; Conti, B.; Conte, U. Cellulose acetate trimellitate ethylcellulose blends for non-steroidal anti-inflammatory drug (NSAID) microspheres. *J. Microencapsulation* **1996**, *13* (1), 89–98.
- (13) Hasegawa, A.; Kawamura, R.; Nakagawa, H.; Sugimoto, I. Physical properties of solid dispersions of poorly water-soluble drugs with enteric coating agents. *Chem. Pharm. Bull.* **1985**, *33* (8), 3429–3435.
- (14) Hasegawa, A.; Kawamura, R.; Nakagawa, H.; Sugimoto, I. Application of solid dispersions with enteric coating agents to overcome some pharmaceutical problems. *Chem. Pharm. Bull.* **1986**, *34* (5), 2183–2190.
- (15) Hasegawa, A.; Nakagawa, H.; Sugimoto, I. Solid dispersion obtained from nifedipine and enteric coating agent. I. Dissolution behavior. [Japanese]. *Yakugaku Zasshi* **1984**, *104* (5), 485–489.
- (16) Hasegawa, A.; Taguchi, M.; Suzuki, R.; Miyata, T.; Nakagawa, H.; Sugimoto, I. Supersaturation mechanism of drugs from solid dispersions with enteric coating agents. *Chem. Pharm. Bull.* **1988**, *36* (12), 4941–4950.
- (17) Kai, T.; Akiyama, Y.; Nomura, S.; Sato, M. Oral absorption improvement of poorly soluble drug using solid dispersion technique. *Chem. Pharm. Bull.* **1996**, *44* (3), 568–571.
- (18) Konno, H.; Taylor, L. S. Influence of different polymers on the crystallization tendency of molecularly dispersed amorphous felodipine. *J. Pharm. Sci.* **2006**, *95* (12), 2692–2705.
- (19) Six, K.; Berghmans, H.; Leuner, C.; Dressman, J.; Van Werde, K.; Mullens, J.; Benoist, L.; Thimon, M.; Meublat, L.; Verreck, G.; Peeters, J.; Brewster, M.; Van Den Mooter, G. Characterization of solid dispersions of itraconazole and hydroxypropylmethylcellulose prepared by melt extrusion, Part II. *Pharm. Res.* **2003**, *20* (7), 1047–1054.
- (20) Takeuchi, H.; Handa, T.; Kawashima, Y. Spherical Solid Dispersion Containing Amorphous Tolbutamide Embedded in Enteric Coating Polymers or Colloidal Silica Prepared by Spray-Drying Technique. *Chem. Pharm. Bull.* **1987**, *35* (9), 3800–3806.
- (21) Takeuchi, H.; Nagira, S.; Yamamoto, H.; Kawashima, Y. Solid dispersion particles of tolbutamide prepared with fine silica particles by the spray-drying method. *Powder Technol.* **2004**, *141* (3), 187–195.
- (22) Tanno, F.; Nishiyama, Y.; Kokubo, H.; Obara, S. Evaluation of hypromellose acetate succinate (HPMCAS) as a carrier in solid dispersions. *Drug Dev. Ind. Pharm.* **2004**, *30* (1), 9–17.
- (23) Yamaguchi, T.; Nishimura, M.; Iguchi, H.; Okamoto, R.; Takeuchi, T.; Yamamoto, K. Improvement of Pharmaceutical Properties of 4'-O-(4-methoxyphenyl)acetyltylosin Using Solid Dispersion with Carboxymethylcellulose. *Yakuzaigaku* **1993**, *53* (4), 221–228.
- (24) Miyajima, M.; Yamaguchi, Y.; Tsunematsu, T.; Oda, T. Pharmaceutical Composition of Dihydropyridine Compound. U.S. Patent 4,983,593, 1991.
- (25) Crew, M. D.; Curatolo, W. J.; Friesen, D. T.; Gumkowski, M. J.; Lorenz, D. A.; Nightingale, J. A. S.; Ruggeri, R. B.; Shanker, R. M. Pharmaceutical compositions of cholesteryl ester transfer protein inhibitors. U.S. Patent 7,235,259, 2007.
- (26) Chiou, W. L.; Riegelman, S. Pharmaceutical applications of solid dispersion systems. *J. Pharm. Sci.* **1971**, *60* (9), 1281–302.
- (27) Kaushal, A. M.; Gupta, P.; Bansal, A. K. Amorphous drug delivery systems: molecular aspects, design, and performance. *Crit. Rev. Ther. Drug Carrier Syst.* **2004**, *21* (3), 133–193.
- (28) Leuner, C.; Dressman, J. Improving drug solubility for oral delivery using solid dispersions. *European Journal of Pharmaceutics & Biopharmaceutics* **2000**, *50* (1), 47–60.
- (29) Serajuddin, A. T. M. Solid dispersion of poorly water-soluble drugs: Early promises, subsequent problems, and recent breakthroughs. *J. Pharm. Sci.* **1999**, *88* (10), 1058–1066.
- (30) Loftsson, T.; Fridriksdottir, H.; Gudmundsdottir, T. K. The effect of water-soluble polymers on aqueous solubility of drugs. *Int. J. Pharm.* **1996**, *127* (2), 293–296.
- (31) Hancock, B. C.; Zografi, G. Characteristics and significance of the amorphous state in pharmaceutical systems. *J. Pharm. Sci.* **1997**, *86* (1), 1–12.
- (32) Yu, L. Amorphous pharmaceutical solids: preparation, characterization and stabilization. *Adv. Drug Delivery Rev.* **2001**, *48* (1), 27–42.

greater than the  $T_g$  of the amorphous pure drug.<sup>7,27,31,33,34</sup> The physical presence of the polymer can also retard the rate of drug crystallization during preparation of the solid dispersion and in storage, as drug molecules are disrupted from interacting within the polymer matrix.<sup>18,34</sup> In some cases, intermolecular interactions between drug and polymer may exist within the polymer phase, further stabilizing the blend.<sup>35</sup>

Hot melt extrusion and spray-drying from organic solvents have emerged as the predominant technologies for preparation of amorphous solid dispersions of poorly soluble drugs at both the laboratory and large scale.<sup>2,4,9,12,17,19,23,36–40</sup> The spray-drying technique is useful for rapidly removing the organic solvent used to dissolve both the drug and matrix polymer, resulting in an amorphous phase. Use of volatile solvents minimizes the processing temperatures used for production of the dry product, which can be of concern for temperature-sensitive compounds in the hot melt extrusion technique. Spray-drying also has the benefits of providing a somewhat uniform particle size, based on the atomization nozzle selection and dryer design.

The vanilloid receptor VR1, identified as a result of its activation by capsaicin, is a cation channel protein expressed by primary sensory neurons termed nociceptors.<sup>41</sup> AMG 517 has been investigated as a potent and selective VR1 antagonist for the treatment of acute and chronic pain. The structure of AMG 517 free base is depicted in Figure 1. The free base is characterized as having very low aqueous solubility ( $\leq 7.0 \mu\text{g/mL}$  over pH 2 to 7;  $< 0.3 \mu\text{g/mL}$  in PBS

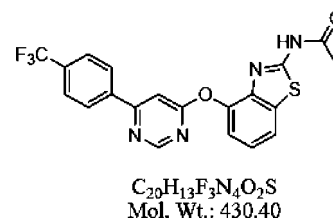


**Figure 1.** Structure of AMG 517.

at pH 7.1) and a high melting point (232 °C). Due to the low  $pK_a$  of the free base, forming of salts having improved solubility proved difficult.

The poor solubility of AMG 517 free base makes it a challenge to develop as a solid dosage form. Ora-Plus vehicle, in combination with a dispersing agent, such as Pluronic, is typically used for preclinical and clinical phase I pharmacokinetic evaluations of small molecule compounds. In early animal exposure studies, improved exposure was attained from a suspension of the micronized free base in 10% w/v Pluronic F108 in OraPlus at lower doses ( $< 10 \text{ mg/kg}$ ). Investigation by Bak et al. revealed the improved exposure in OraPlus was actually due to the formation of a cocrystal between AMG 517 and sorbic acid, a preservative in OraPlus.<sup>42</sup> At higher doses ( $> 30 \text{ mg/kg}$ ), solubility-limited absorption was still observed with the OraPlus suspension.

In the present study, we investigate application of an amorphous solid dispersion (ASD) formulation approach to provide a solid dosage form with improved in vivo exposure of AMG 517 over its free base suspended in an OraPlus vehicle. ASD particles are formed from organic solvent solutions of drug and codissolved hydrophilic carrier polymers using a spray-drying technique. Hydroxypropyl methylcellulose (HPMC-E5) and hydroxypropyl methylcellulose acetate succinate (HPMCAS-MF) were selected as matrix polymers. Each polymer has been studied previously for use in solid dispersions, and each has particular advantage both for processing by spray-drying and in promoting stability due to their high glass transition temperatures ( $T_g$ ).<sup>17,18,22–25</sup>

HPMCAS is an enteric polymer, its acetyl and succinoyl groups affording control over its dissolution behavior at different pH. This feature could have advantage in delaying gelation and dissolution of the ASD matrix until the formulation reaches the small intestine, thus better maintaining a high degree of drug supersaturation within the absorptive region of the GI tract. HPMCAS also has a lower degree of moisture uptake compared to HPMC, which may impact storage stability of the ASD by decreasing the plasticization effect of water. The variation in functional groups between HPMC and HPMCAS are also likely to affect the drug's ability to interact with the polymer via hydrogen bonding or hydrophobic interactions, with a

- (33) Saleki-Gerhardt, A.; Zografi, G. Non-isothermal and isothermal crystallization of sucrose from the amorphous state. *Pharm. Res.* **1994**, *11* (8), 1166–1173.
- (34) Shamblin, S. L.; Huang, E. Y.; Zografi, G. The effects of co-lyophilized polymeric additives on the glass transition temperature and crystallization of amorphous sucrose. *J. Therm. Anal.* **1996**, *47* (5), 1567–1579.
- (35) Taylor, L. S.; Zografi, G. Spectroscopic characterization of interactions between PVP and indomethacin in amorphous molecular dispersions. *Pharm. Res.* **1997**, *14* (12), 1691–1698.
- (36) Nakamichi, K.; Nakano, T.; Izumi, S.; Yasuura, H.; Kawashima, Y. The preparation of enteric solid dispersions with hydroxypropylmethylcellulose acetate succinate using a twin-screw extruder. *J. Drug Delivery Sci. Technol.* **2004**, *14* (3), 193–198.
- (37) Nakamichi, K.; Yasuura, H.; Fukui, H.; Oka, M.; Izumi, S.; Andou, T.; Shimizu, N.; Ushimaru, K. Preparation of nifedipine-hydroxypropylmethylcellulose phthalate solid dispersion by twin screw extruder and its evaluation. *Yakuzaigaku* **1996**, *56* (1), 15–22.
- (38) Otsuka, M.; Onoe, M.; Matsuda, Y. Hygroscopic stability and dissolution properties of spray-dried solid dispersions of furosemide with Eudragit. *J. Pharm. Sci.* **1993**, *82* (1), 32–8.
- (39) Verreck, G.; Six, K.; Van Den Mooter, G.; Baert, L.; Peeters, J.; Brewster, M. E. Characterization of solid dispersions of itraconazole and hydroxypropylmethylcellulose prepared by melt extrusion: Part I. *Int. J. Pharm.* **2003**, *251* (1–2), 165–174.
- (40) Beyerinck, R. A.; Diebele, H.; Dobry, D.; Ray, R.; Settell, D.; Spence, K. Method for making homogeneous spray-dried solid amorphous drug dispersions utilizing modified spray-drying apparatus. U.S. Patent 6,973,741, 2005.
- (41) Julius, D.; Basbaum, A. I. Molecular mechanisms of nociception. *Nature* **2001**, *413* (6852), 203–210.

- (42) Bak, A.; Gore, A.; Yanez, E.; Stanton, M.; Tufekci, S.; Syed, R.; Akrami, A.; Rose, M.; Surapaneni, S.; Bostick, T.; King, A.; Neervannan, S.; Ostovic, D.; Koparkar, A. The co-crystal approach to improve the exposure of a water-insoluble compound: AMG 517 sorbic acid co-crystal characterization and pharmacokinetics. *J. Pharm. Sci.* **2008**, *97* (9), 3942–3956.



potential impact on both solid-state stability and in vivo performance. Amorphous solid dispersions were formed at low (15 wt %) and high (50 wt %) drug loads and initially characterized to verify formation of amorphous, dry powders. Practical consideration was given toward exploring compositions that could ultimately provide a solid dosage form at a strength relevant to the range explored in recent human clinical trials.<sup>43</sup> ASD powders were then subjected to stability testing under open conditions at elevated temperature and humidity (40 °C/75% RH) for up to six months. In vitro dissolution testing screened the concentration-enhancement features of ASD powders in a supersaturated system, and intrinsic dissolution characteristics were determined for the highest ranking ASD powder. Pharmacokinetics of an AMG 517 formulation, prepared in a capsule using the highest ranking ASD powder, was evaluated in cynomolgus monkeys and compared with AMG 517 free base suspended in OraPlus.

## Experimental Section

**Materials.** AMG 517 micronized free base (Lot # 9902174) was synthesized in-house. Hydroxypropyl methylcellulose acetate succinate, “AQOAT AS-MF” (HPMCAS-MF), was obtained from Shin Etsu Chemical Company (Tokyo, Japan). Hydroxypropyl methylcellulose, “Methocel E5 Premium LV”, (HPMC-E5) was obtained from Dow Chemical Company (Midland, MI). Pluronic F108 (Lot # WPAY635B) was obtained from BASF (Florham Park, NJ). Ora-Plus (Lot # 6267276) was obtained from Paddock Laboratories Inc. (Minneapolis, MN).

Methyl acetate (minimum 99%) was obtained from Alfa Aesar (Ward Hill, MA). Methanol (minimum 99.5%) and ethyl acetate (minimum 99.5%) were obtained from Mallinckrodt Baker Inc. (Phillipsburg, NJ). All other excipients and chemicals from vendors were either pharmaceutical NF or reagent grade, and were used as received.

**Preparation of Spray-Dried Amorphous Solid Dispersions.** Polymers HPMCAS-MF and HPMC-E5 were dissolved in ethyl acetate (HPMCAS-MF) or 50:50 v/v methyl acetate:methanol (HPMC-E5) at 20 mg/mL. Polymer solutions were added to AMG 517 micronized free base to form solutions containing 50:50 or 85:15 w/w of polymer to drug. AMG 517 solubility in ethyl acetate and 50:50 methyl acetate:methanol were previously determined as ~30 mg/mL and >20 mg/mL, respectively. Solutions were spray-dried at 0.75 mL/min using a Büchi 290 spray-dryer (Brinkmann Instruments, Inc., Westbury, NY) specially equipped with a 48 KHz ultrasonic atomizing nozzle (Sono-Tek Corp., Milton, NY). The spray-dryer was configured with

an inert N<sub>2</sub> gas feed in open cycle mode and the aspirator was bypassed; the drying gas flow rate was 300 slpm. Exhaust was routed to a vented exhaust manifold. For ethyl acetate, the inlet N<sub>2</sub> temperature was 75 °C; for methyl acetate/methanol the inlet temperature was either 45 or 50 °C. The atomizing nozzle was supplied with focusing N<sub>2</sub> at 30 slph; power to the nozzle was approximately 2 W.

Following spray-drying, the amorphous solid dispersion powder was collected into vials, sealed, and stored under desiccant at 4 °C until analysis or use. The effect of secondary drying in a vacuum oven (80 °C/84 h) was assessed for one lot of the amorphous solid dispersion formulations (HPMCAS, 15 wt % AMG 517, Lot 2); this secondary dried material was subsequently used in the pharmacokinetic study.

**Initial Characterization. (a) Scanning Electron Microscopy (SEM).** A thin layer of dry particles were placed on the adhesive surface of a carbon conductive tab adhered to a pin stub SEM mount (Ted Pella, Redding, CA) and sputter-coated under argon with a thin layer of gold–palladium using a Pelco SC-7 (Ted Pella, Redding, CA) sputter coater unit. For freeze-fracture SEM analysis of internal particle morphology, particles were sandwiched between two adhesive stubs, chilled in liquid nitrogen, and rapidly separated to produce two fracture surfaces for sputter-coating. Samples were imaged using a Philips XL30 ESEM TMP scanning electron microscope (Philips, FEI Company, Hillsboro, OR), operating at an acceleration voltage of 5 kV. Images were captured with analysis XL Docu software (Soft Imaging Systems, Lakewood, CO).

**(b) Particle Size Analysis.** Particle size was measured using a Malvern Mastersizer 2000 equipped with a Hydro 2000  $\mu$ P wet dispersion cell (Malvern Instruments Ltd., Worcestershire, U.K.). Approximately 10 mg of particles was dispersed in 0.5 mL of Sedisperse A-12 (Micromeritics Corp., Norcross, GA), and added to the dispersion cell containing hexane. Particle size distribution was calculated using the Mie theory optical diffraction model<sup>44</sup> (particle refractive index and absorption estimated at 1.500 and 0.001, respectively) to yield the volume based diameter parameters at 10%, 50%, and 90% cumulative volume percent:  $d[v,0.1]$ ,  $d[v,0.5]$ , and  $d[v,0.9]$ .

**(c) Determination of Free Base Content.** AMG 517 content within HPMCAS and HPMC-E5 solid dispersion microparticles was quantified by high-performance liquid chromatography (HPLC). Samples were prepared in acetonitrile/water (50/50, v/v), with AMG 517 reference standard lot 0502L740, prepared at 0.125 mg/mL, as the calibration standard for quantitation. A Phenomenex Luna 5  $\mu$  C18(2), 150 mm  $\times$  4.6 mm, 5  $\mu$ m, 100A (Phenomenex, P/N 00F-4252-E0) analytical column was used, with a mobile phase consisting of acetonitrile, water and trifluoroacetic acid (80:20:0.1). A gradient elution method at 1 mL/min was employed, with detection at 254 nm via a HP1100 diode

(43) Gavva, N. R.; Treanor, J. J. S.; Garami, A.; Fang, L.; Surapaneni, S.; Akrami, A.; Alvarez, F.; Bak, A.; Darling, M.; Gore, A.; Jang, G. R.; Kesslak, J. P.; Ni, L.; Norman, M. H.; Palluconi, G.; Rose, M. J.; Salfi, M.; Tan, E.; Romanovsky, A. A.; Banfield, C.; Davar, G. Pharmacological blockade of the vanilloid receptor TRPV1 elicits marked hyperthermia in humans. *Pain* **2008**, *136* (1–2), 202–210.

(44) van de Hulst, H. C. *Light Scattering by Small Particles*; Dover Publications: New York, 1981.

array detector (Agilent HP1100 G1315B). Loading efficiency (LE %) within the amorphous solid dispersion was defined as:  $LE \% = [(determined\ wt \% AMG\ 517) \div (theoretical\ wt \% AMG\ 517)] \times 100\%$ .

**(d) Thermal Analysis.** Mass-loss properties were characterized using a TGA Q500 (TA Instruments, New Castle, DE). Modulated DSC (MDSC) was performed on a DSC Q1000 by TA Instruments. Data analysis utilized Universal Analysis 2000 thermal analysis software by TA Instruments. Samples were allowed to equilibrate to room temperature in sealed vials prior to sample preparation. For TGA, samples of 2–6 mg were heated at 10 °C/min over a temperature range of 10 to 300 °C. For MDSC, samples of 2–3 mg were weighed and placed in aluminum crimped pans. MDSC parameters were modulated at  $\pm 1.00$  °C every 60 s with heating rates of 3.00 °C/min from –10 °C to 200–250 °C. Measurements were performed under nitrogen purge.

**(e) X-ray Powder Diffraction (XRPD).** X-ray diffraction patterns were obtained using a Phillips automated X-ray powder diffractometer, X'Pert PRO (PANalytical, Almelo, Netherlands). A Cu K $\alpha$  X-ray tube (PW337310 LFF, 1.54 Å) was used with voltage and current of 45 kV and 40 mA, respectively. The incident path was set with a 0.04 rad solar slit, 15 mm fixed mask, 1/2° fixed antiscatter slit, and a 1/4° fixed divergence slit. The diffracted beam path detected by the RTMS detector/X'Cellerator, was set with a 0.04 rad solar slit, 0.09° parallel plate collimator, and 0.02 mm nickel filter. Samples of 5–10 mg were prepared on the sample holder and the stage rotated over the range of  $2\theta$  from 3° to 40°. High resolution scans of about 6 h were collected.

**Stability Study.** The stability of ASD formulations was monitored up to 6 months at elevated temperature and relative humidity. Samples were placed in the humidity chamber at 40 °C/75% RH (open dish). Periodically samples were removed and characterized by XRPD.

**Dissolution Studies.** Dissolution screening was performed on Vankel VK7000 dissolution station equipped with a USP 2 (paddle) apparatus and 200 mL Varian mini-vessels (P/N 12-5050). Samples were manually drawn through 10  $\mu$ m filters (Varian 10  $\mu$ m cannula filters, UHMW polyethylene 17-4000, FIL010-01-100)) using a 3 mL syringe attached with a sampling cannula (CAN475-HR, 4.75", Hansen Research).

The dissolution profiles of AMG 517 amorphous solid dispersion samples (powder and capsules) were studied in 100 mL of pH 6.8 phosphate buffer at a paddle rotation of 100 rpm, with a constant temperature bath at  $37 \pm 0.5$  °C. Powder samples were weighed into a paper boat, while capsule samples (as prepared below) were placed into Sortax sinkers. Each test system used 12.5 mg of drug. Samples were then dropped into the dissolution vessel to start the dissolution experiment. 1.5 mL samples were drawn at 5, 10, 15, 30, 45, 60, 90 and 120 min with no dissolution medium replacement, and the sample was transferred to a 2 mL HPLC autosampler vial for analysis. AMG 517 was quantified by HPLC, using a method similar to that described above.

The intrinsic dissolution rate was determined using a stationary disk with the USP 2 apparatus equilibrated at 37 °C, with a paddle speed of 100 rpm. 0.8 cm disks were produced by compression using a benchtop press at ~2000 psi for 1 min. The dissolution medium was 900 mL of pH 6.8 phosphate buffer with 2% SDS.

**Pharmacokinetic Study. (a) Preparation.** All investigations using experiment animals adhered to the "Principles of Laboratory Animal Care" (NIH publication #85-23, revised in 1985). The pharmacokinetic study of AMG 517 was conducted in fasted male cynomolgus monkeys ( $n = 6$ ) in a crossover study design comparing an AMG 517 Ora-Plus aqueous suspension to an ASD formulation dosed within a capsule. The body weight of the monkeys ranged from 3 to 4 kg; a fixed dose of AMG 517 of 12.5 mg was given to individual animals. Wash-out time between each dosing phase of the study was 13 days.

Preparation of the Ora-Plus aqueous suspension began by combining 20 g of Pluronic F108 to 200 mL of OraPlus and stirring overnight at room temperature. 150.0 g of the 10% Pluronic F108 in OraPlus vehicle was added to a bottle containing 150.1 mg of AMG 517 micronized free base in a 250 mL Pyrex bottle. The components were mixed using a homogenizer probe for 3 min until the suspension appeared uniform. Final suspension concentration was approximately 1 mg/mL. For the ASD formulation, 950 mg of powder was added to a vial with 50 mg of sodium dodecyl sulfate, and the contents intimately mixed using a vortex mixer. Approximately 85 mg of the mixture was filled into size 1 gelatin capsules.

AMG 517 aqueous suspension in the 10% pluronic F108/Ora-Plus vehicle was administered via oral gavage intubation, followed by a flush of approximately 10 mL of air to clear the gavage tube. The ASD formulation blend in capsule (HPMCAS, 15 wt % AMG 517, Lot 2 + 5 wt % SDS) was administered orally, and 15 mL of water was provided to each monkey as flush liquid after capsule administration.

For each phase of the study, approximately 1 mL of blood was collected from each animal via the femoral vein into 3 mL tubes containing lithium heparin anticoagulant at predose, and following oral dose administration at 0.5, 1, 2, 4, 8, 12, 24, 30, 48, 72, 96, 120, 192, 216, and 240 h postdose. Blood tubes were inverted 10–15 times and stored on ice prior to centrifugation (14000g for 2 min) to obtain plasma. Plasma (approximately 500  $\mu$ L) was transferred to separate tubes and stored at –10 °C or below until analysis.

**(b) Bioanalytical Method for Pharmacokinetic Studies.** Lithium heparinized male cynomolgus monkey plasma samples (50  $\mu$ L) were extracted using 96-well liquid/liquid extraction (LLE) to isolate the analyte and internal standard. Samples were separated by reversed-phase liquid chromatography on a Thermo Electron Hypersil BDS C18,  $50 \times 2.1$  mm (5  $\mu$ m) analytical column. The mobile phase was 75:25 MeOH:10 mM ammonium acetate in water (mobile phase B). An isocratic of mobile phase B at a flow rate of 450  $\mu$ L/min was utilized, with a total run time of 4.0 min.

**Table 1.** Characterization Summary for ASD Formulations of AMG 517 Prepared from HPMCAS-MF and HPMC-E5 by Spray-Drying

formulation ID	polymer	drug (wt %)	yield (%)	LE <sup>a</sup> (%)	$d_{50}^b$ ( $\mu\text{m}$ )	% wt loss by TGA	$T_g$ ( $^{\circ}\text{C}$ ) by MDSC
A, Lot 1	HPMCAS-MF	15	76		34.2	2.39	106
A, Lot 2		15	85	98.8	35.3 <sup>c</sup>	0.32 <sup>c</sup>	101 <sup>c</sup>
B		50	55	97.5	40.7	2.84	98
C		15	61	99.1	34.6	1.94	117
D, Lot 1		50	12 <sup>d</sup>	99.0	34.6	1.88	106
D, Lot 2	HPMC-E5	50	60		28.7	1.44	107

<sup>a</sup> Load efficiency (LE). <sup>b</sup> Particle size diameter at 50% cumulative volume %. <sup>c</sup> For "A, Lot 2", results are provided for material after secondary drying in a vacuum oven. <sup>d</sup> Inlet drying temperature was 45  $^{\circ}\text{C}$ .

A related molecule, AMG1664, was used as the internal standard. Plasma calibration curve standards were prepared at concentrations of 0.500, 1.00, 2.50, 5.00, 10.0, 25.0, 50.0, 100, 250, 500 and 1000 ng of AMG 517/mL of lithium heparinized male cynomolgus monkey plasma.

AMG 517 concentrations were determined in lithium heparinized male cynomolgus monkey plasma samples by LC–MS/MS using ion atmospheric pressure chemical ionization (APCI) with multiple reaction monitoring (MRM) in the positive ion mode. Peak areas were integrated by the Sciex program Analyst, version 1.4.1, residing on a Windows 2003 computer. Following peak area integration, the data was exported to the software Watson (PROD) (version 7.0.0.01, InnaPhase Corp., Philadelphia, PA) where concentrations were determined by a weighted ( $1/x^2$ ) linear regression of peak area ratios (peak area of AMG 517/peak area of AMG1664) versus the theoretical concentrations of the plasma calibration standards. Calculations were performed on unrounded numbers. Overall precision and accuracy for the calibration standards and QC samples were determined by Watson (PROD). Study sample concentrations were rounded to three decimal places before reporting.

**(c) Pharmacokinetic Analysis.** Individual plasma concentration–time data were analyzed by noncompartmental methods using WinNonlinTM v. 4.1e Build 200408051632 (Pharsight Corporation, Mountain View, CA). Nominal sampling times were used in the pharmacokinetic analysis; actual times were all  $\pm 10\%$  of the respective nominal time. The area under the concentration–time curve from time zero to infinity ( $\text{AUC}_{0-\text{inf}}$ ) was calculated using the linear–log trapezoidal method. The maximum plasma concentration ( $C_{\text{max}}$ ) observed and the time at which it was observed ( $T_{\text{max}}$ ) were determined directly from the individual plasma concentration–time profiles. Relative bioavailability ( $F_{\text{rel}}$ ) was calculated by comparing exposures from the capsule formulation to the standard Ora-Plus suspension formulation.

## Results

**Preparation of ASD Material by Spray-Drying.** Formulations produced by spray-drying are summarized in Table 1. Formulations produced from HPMCAS appeared as a white, dry, fine powder in the product collector. Collection yield values were high based on the quantities produced. For formulation A, batch sizes of 8 g (Lot 1) and 6 g (Lot 2) gave yields of 76% and 85%, respectively. For formulation

B, a batch size of only 2 g gave a yield of 55%. Generally, yields will be impacted at lower batch sizes due to fixed losses within the dryer. The yield values obtained are in line with typical production yields from easily dried materials, based on our experience with the laboratory-scale dryer.

As described, the effect of secondary drying in a vacuum oven (80  $^{\circ}\text{C}$ /84 h) was assessed for formulation A, Lot 2. After drying, the secondary-dried material still appeared as a white, fine powder. The secondary dried form of A, Lot 2 was subsequently characterized as described below.

Spray-drying of formulations with HPMC-E5 began chronologically with formulation D, Lot 1, for which the inlet temperature was 45  $^{\circ}\text{C}$  and the outlet temperature of the dryer was 32  $^{\circ}\text{C}$ . Collection yield for this initial lot was only 12% for a 3 g batch size, and observations suggested heavy accumulation of sprayed material within the dryer column. Thus, inlet temperature was increased to 50  $^{\circ}\text{C}$  for subsequent formulations of HPMC-E5. Yield values, as a result, improved to 60%, for a 3 g batch size (D, Lot 2). Spray-drying of formulation C, at a 2 g batch size, produced a yield of 61%, in line with the aforementioned yields obtainable in the dryer.

The drug load efficiency in spray-dried ASD formulations of AMG 517 are indicated in Table 1. As expected, loading efficiency was near 100% for all formulations. Values were not adjusted for the minor levels of residual solvents within the particles (see TGA results, below).

**Initial Characterization. (a) SEM.** Representative SEM micrographs of the 15 wt % AMG 517 solid dispersions prepared from HPMCAS are presented in Figures 2A and 2B, while a micrograph of the 15 wt % AMG 517 solid dispersions prepared from HPMC-E5 is presented in Figure 2C. The low resolution images (Figure 2A) shows the particles to be predominantly disperse and irregularly shaped, with sizes ranging over about 10–60  $\mu\text{m}$ . Higher resolution images (Figure 2B, Figure 2C) suggest the irregular shape is a result of a dense skin forming at the surface of an evaporating droplet and subsequently collapsing upon itself during drying, much like a raisin. Electron micrographs for 50 wt % AMG 517 solid dispersions (not shown) appeared similar.

A freeze-fracture SEM micrograph of HPMCAS formulations containing 15 wt % AMG 517 is presented in Figure 2D (50 wt %, not shown, appeared similar). Internal morphology of the collapsed structures appears as a smooth,



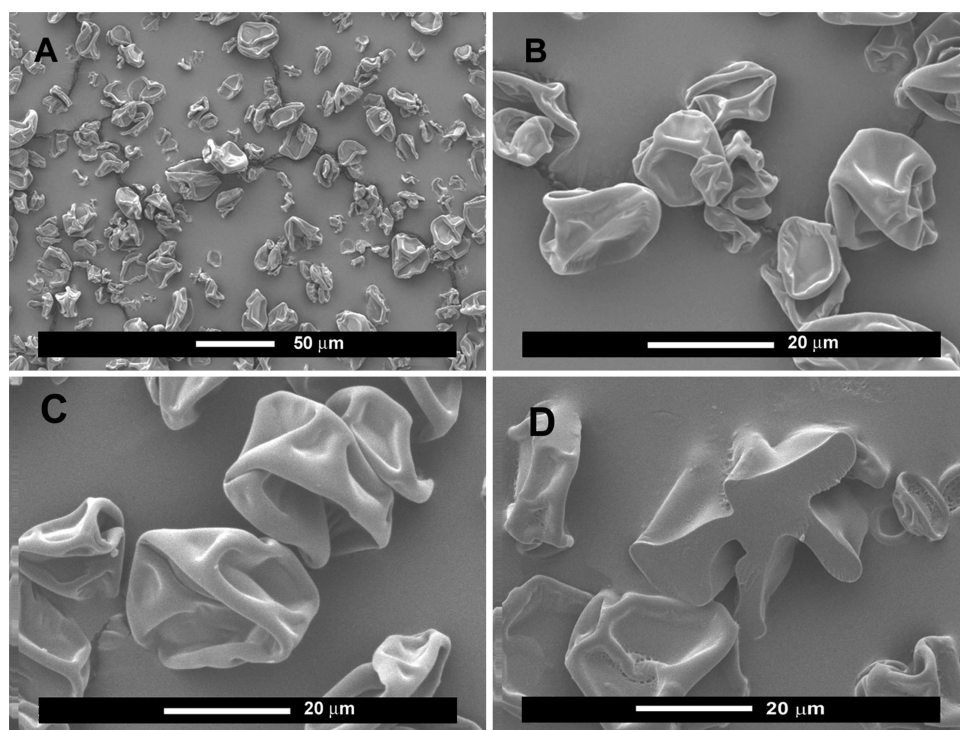


**Figure 2.** SEM micrographs of ASD formulations: (A) formulation “A, Lot 2” (15 wt % AMG 517 in HPMCAS), 402 $\times$ ; (B) formulation “A, Lot 2” (15 wt % AMG 517 in HPMCAS), 1609 $\times$ ; (C) formulation “C” (15 wt % AMG 517 in HPMC-E5), 1609 $\times$ ; (D) freeze-fracture SEM micrograph of formulation “A, Lot 2” (15 wt % AMG 517 in HPMCAS), 1508 $\times$ .

solid monolithic structure, devoid of any pores or macrovoids. The lack of any observable crystalline structure in the surface or internal SEM micrographs supports the presence of an amorphous form of the drug.

**(b) Particle Size.** Median particle size (volume based diameter parameter,  $d[v,0.5]$ ) for formulations produced by spray-drying are summarized in Table 1. The results agree with the qualitative assessment of the SEM micrographs. The median size,  $d[v,0.5]$ , was similar across the formulations, with  $d[v,0.5]$  ranging from 29 to 41  $\mu\text{m}$ . The 10% cumulative volume diameter ( $d[v,0.1]$ ) and 90% cumulative volume parameter ( $d[v,0.9]$ ) ranged from 15 to 21  $\mu\text{m}$  and 52 to 75  $\mu\text{m}$ , respectively.

For formulation A, Lot 2, the distribution parameters following secondary drying were similar to the particle size of the same formulation (A, Lot 1) measured immediately after spray-drying. Thus, secondary drying at 80  $^{\circ}\text{C}$  did not lead to significant particle agglomeration.

**(c) Thermal Analysis.** Thermogravimetric analysis (TGA) was performed on initially formed spray-dried ASD formulations to gauge residual solvent content (Table 1). The method was not distinguishing between the residual polymer solvent and moisture uptake within the as-prepared formulations. Manufacturer literature for HPMC-AS suggests moisture can be on the order of 2%–5% for pure polymers after storage at 40–60% RH; moisture levels for HPMC-E5 over the same % RH range are on the order of 4%–8%. Values from Table 1 indicate weight loss values on the order of 1% to 3% across formulations, within or slightly below the limits of typical moisture absorption for pure polymers. Although particles

were formed from an organic-solvent solution in dry nitrogen, it is expected that at least a portion of the TGA weight loss is a result of moisture. The presence of the hydrophobic drug may also decrease moisture uptake over the pure-polymer values. The values in Table 1 thus set an upper bound for polymer solvent content. Headspace-GC analysis for HPM-CAS formulations, produced previously, indicated ethyl acetate solvent content was approximately 3%, consistent with TGA weight loss values (data not shown). Formulation A, Lot 2, had lower weight loss by TGA following secondary drying in a vacuum oven at 80  $^{\circ}\text{C}$ , likely indicating the removal of residual ethyl acetate (and/or moisture). Spray-drying at a higher dryer inlet temperature had an impact on weight loss by TGA: formulation D, Lot 1, exhibited higher weight loss by TGA compared with formulation D, Lot 2.

TGA weight loss curves over the range 25–225  $^{\circ}\text{C}$  are presented in Figure 3 for HPMCAS formulations (A, Lot 1 and B), and HPMC-E5 formulations (C and D, Lot 2). Weight loss by solvent/moisture loss occurs primarily over the range from 25  $^{\circ}\text{C}$  to about 150  $^{\circ}\text{C}$ . Secondary drying conditions (80  $^{\circ}\text{C}$ ) were based on the observed loss curves to maximize the rate of solvent removal, yet maintain physical stability by drying at least 20  $^{\circ}\text{C}$  below the  $T_g$  of the formulation (see MDSC results, below).

MDSC measurements for all formulations indicated single glass transitions over the entire range of the measurements (Figure 3). The results suggest the drug and polymers formed uniform solid dispersions at the compositions studied. Melting point of AMG 517 free base (form A) is reported as 229  $^{\circ}\text{C}$ ; MDSC analysis of pure amorphous AMG 517

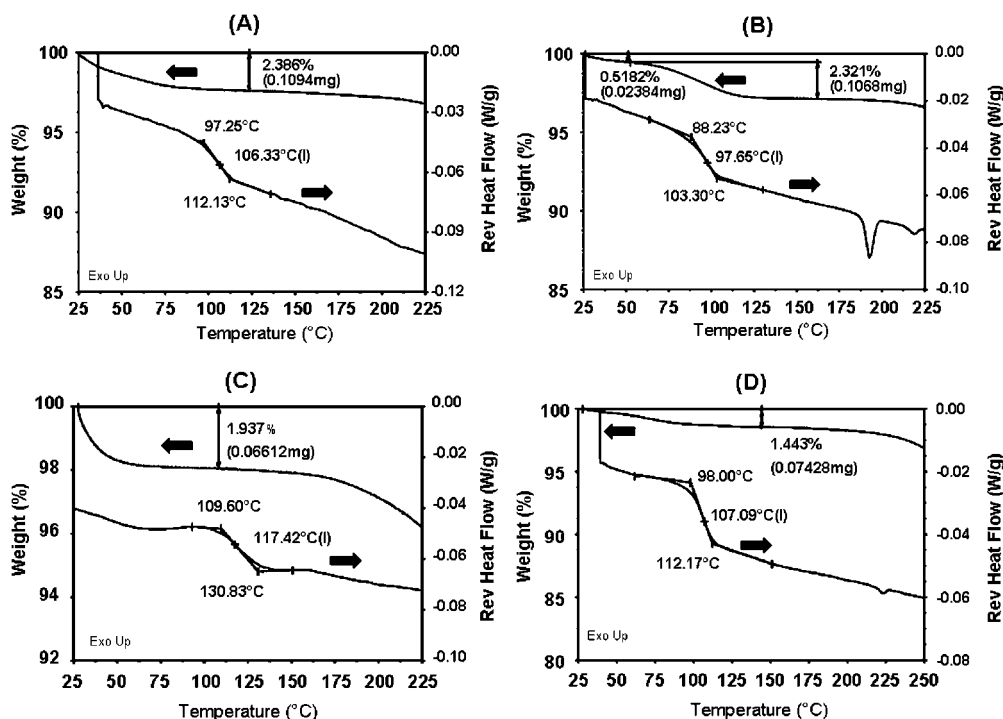


**Figure 3.** Thermal analysis (TGA and MDSC) of amorphous solid dispersions, as initially formed: (A) formulation “A, Lot 1”, 15 wt % AMG 517, HPMCAS; (B) formulation “B”, 50 wt % AMG 517, HPMCAS; (C) formulation “C”, 15 wt % AMG 517, HPMC-E5; (D) formulation “D, Lot 2”, 50 wt % AMG 517, HPMC-E5.

produced by spray-drying (not shown), gave a single  $T_g$  at 103 °C ( $\Delta C_p = 0.42 \text{ J/g}^\circ\text{C}$ ). The endotherm in the MDSC plots for the 50 wt % HPMCAS formulation at  $\sim 190^\circ\text{C}$  (Figure 3B) corresponds to melting of a polymorph, as a broad recrystallization exotherm in the total heat flow curve was observed between  $\sim 160^\circ\text{C}$  and  $\sim 180^\circ\text{C}$  (not shown). Similar endothermic transitions were observed for the 50% HPMC-E5 formulations near  $220^\circ\text{C}$ , suggesting both formulations containing 50% drug experienced devitrification upon heating beyond their respective glass transition temperatures. Numerical values for the  $T_g$  of each lot produced are summarized in Table 1.

**(d) X-ray Powder Diffraction.** X-ray powder diffraction (XRPD) profiles of initially formed spray-dried formulations from HPMCAS and HPMC-E5 are presented in Figure 4. All formulations, analyzed over 6 h, show a halo in XRPD characteristic to the amorphous form. The small peak at  $2\theta \sim 27^\circ$  within HPMC-E5 formulations at 50 wt % AMG 517 (Figure 4B) are likely anomalies caused by foreign material and do not correspond to any peaks observed within the XRPD profile of AMG 517 free base (Figure 5, I). Secondary drying of formulation A, Lot 2, under vacuum at  $80^\circ\text{C}$  for greater than 3 days (Figure 4A, II), did not change the XRPD profile.

**(e) Stability Study.** Physical stability of ASD formulations, under open conditions at  $40^\circ\text{C}/75\% \text{ RH}$ , was assessed by XRPD for 6 months (Figure 6). XRPD profiles for HPMCAS formulations at both 15 wt % and 50 wt % AMG 517 show a halo characteristic to the amorphous form after long-term storage (Figure 6 I, II). For HPMC-E5, the 50 wt % AMG 517 formulation was also predominantly X-ray

amorphous (Figure 6, III); a small peak at  $2\theta \sim 33^\circ$  correlates to a minor peak within the AMG 517 free base profile (Figure 5, I). In contrast, highly amorphous AMG 517 produced by spray-drying (Figure 5, II) shows a tendency toward crystallization after only 15 days storage at  $40^\circ\text{C}/75\% \text{ RH}$  (Figure 5, III).

Physical and chemical assay of A, Lot 1 was assessed after 23 months storage at ambient temperature under desiccant. The sample was still X-ray amorphous. Assay value of A, Lot 1 (15% AMG 517 in HPMCAS), previously not measured at time 0 (Table 1), was determined to have a load efficiency (LE) of 100.1%. Percent main peak area was 98.0%, as compared to an AMG 517 standard with percent main peak of 98.5%. Thus, only minor (0.5%) impurities were seen to develop over 23 months at ambient conditions for the formulations.

**Dissolution Study.** Cellulose ethers such as hydroxypropyl methylcellulose (HPMC) and hydroxypropyl methylcellulose acetate succinate (HPMCAS) of the type used in our experiments are typically used in aqueous-soluble film coating applications. Each has been extensively evaluated as carriers for amorphous solid dispersions.<sup>18,19,22,23,25,36,37</sup> HPMC-E5, a nonenteric polymer, is generally soluble in water, is nonionic, and is not expected to have a pH-dependent solubility. The acetyl and succinoyl moieties on HPMCAS render it insoluble in pure water and acidic

(45) Streubel, A.; Siepmann, J.; Peppas, N. A.; Bodmeier, R. Bimodal drug release achieved with multi-layer matrix tablets: transport mechanisms and device design. *J. Controlled Release* **2000**, *69* (3), 455–468.



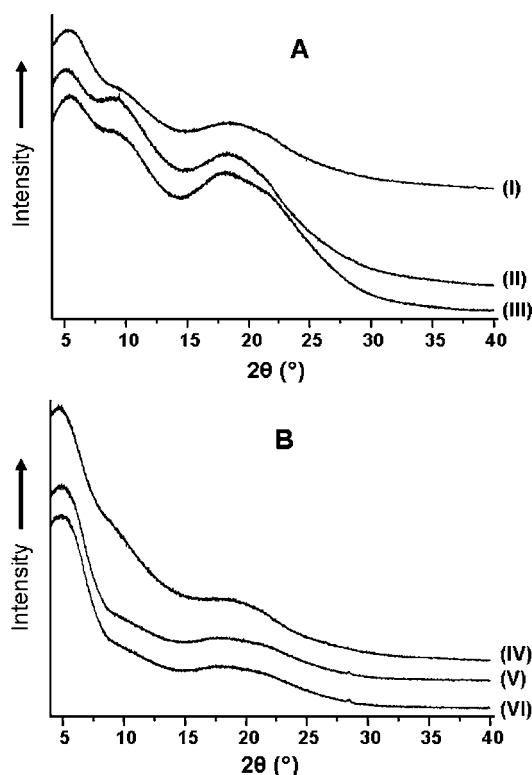


**Figure 4.** XRPD profiles of spray-dried formulations as initially characterized: (A, I) formulation “A, Lot 1”, 15 wt % AMG 517, HPMCAS; (A, II) formulation “A, Lot 2”, 15 wt % AMG 517, HPMCAS, post secondary drying; (A, III) formulation “B”, 50 wt % AMG 517, HPMCAS; (B, IV) formulation “C”, 15 wt % AMG 517, HPMC-E5; (B, V) formulation “D, Lot 1”, 50 wt % AMG 517, HPMC-E5; (B, VI) formulation “D, Lot 2”, 50 wt % AMG 517, HPMC-E5.

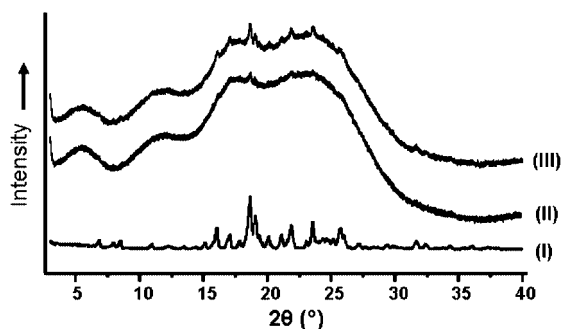


**Figure 5.** XRPD profiles of AMG 517 free base: (I) micronized free base (“form A”); (II) substantially amorphous free base, as initially formed by spray-drying from ethyl acetate; (III) substantially amorphous free-base, after storage at 40 °C/75% RH for 15 days under open conditions.

environments, enabling its use as an enteric coating polymer.<sup>45</sup> HPMCAS-MF is characterized as having increased solubility above pH 6.5. Kai has demonstrated relative differences in the dissolution behavior at low pH (1.2) and neutral pH (6.8) for solid dispersions of HPMC and a similar enteric polymer, HPMCP.<sup>17</sup> Kai’s results suggest attenuated drug dissolution in low pH for the enteric solid dispersions,

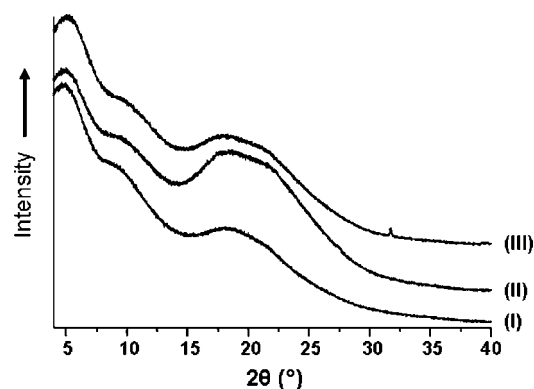


**Figure 6.** XRPD profiles of spray-dried formulations after 6 months under open conditions at 40 °C/75% RH: (I) formulation “A, Lot 1”, 15 wt % AMG 517, HPMCAS; (II) formulation “B”, 50 wt % AMG 517, HPMCAS; (III) formulation “D, Lot 1”, 50 wt % AMG 517, HPMC-E5.

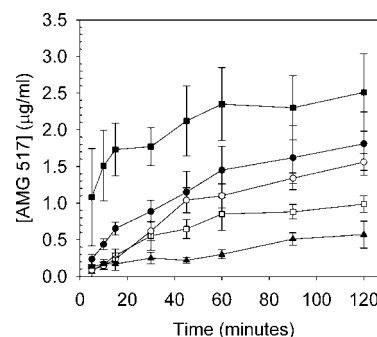


**Figure 7.** Powder dissolution profiles of AMG 517 under saturation conditions in 100 mL of phosphate buffer, pH 6.8 (12.5 mg drug): (■) ASD formulation A, Lot 2 (15 wt % AMG 517 in HPMCAS); (□) ASD formulation B (50% AMG 517 in HPMCAS); (●) ASD formulation C (15% AMG 517 in HPMC-E5); (○) ASD formulation D, Lot 1 (50% AMG 517 in HPMC-E5); (▲) AMG 517 free base, micronized.

while the HPMC dissolution profile was pH-invariant. During our method development, HPMCAS formulations exhibited poor wettability and reduced dissolution in pH 1.2 and water. Thus, to gauge potential performance in vivo, pH 6.8 phosphate buffer was selected as the dissolution medium for the ASD formulations produced by HPMCAS and HPMC.<sup>22</sup>

Dissolution profiles of ASD formulations as powders, over 120 min, under saturation conditions, are shown in Figure 7. For the ASD powders, dissolution concentration over two hours increased 2- to 5-fold over micronized AMG 517 free base. At 15 wt % AMG 517, the ASD powder containing HPMCAS (A, Lot 2) showed greater dissolution than that made in HPMC-E5 (C). For each polymer, ASD formulations show a clear trend of better dissolution with low drug load, e.g. 15% drug loading showed better dissolution than that of 50%. A higher amount of swellable polymers in the 15% wt % AMG 517 formulations will increase the amount of water uptake in the ASD sample, and therefore increases the wetting of the drug, leading to a greater dissolution compared to formulations with lower polymer content. There was a wider disparity between results for HPMCAS,

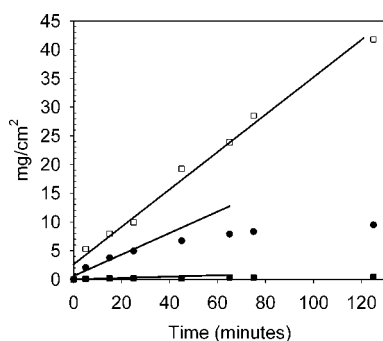


**Figure 8.** Intrinsic dissolution profiles fit by linear regression for slope ( $m$ ) and intercept ( $b$ ): (□) ASD formulation A, Lot 2 (15 wt % AMG 517 in HPMCAS) with correction for load (fit:  $m = 0.33$ ,  $b = 2.62$ ,  $R^2 = 0.98$ ); (■) AMG 517 free base (fit:  $m = 0.0115$ ,  $b = 0.013$ ,  $R^2 = 0.96$ ); (●) amorphous AMG 517 (fit:  $m = 0.187$ ,  $b = 0.583$ ,  $R^2 = 0.94$ ).

compared with HPMC. Analysis of the suspended solid by XRD, following dissolution, was not performed. Nevertheless, the profiles in Figure 7 indicate increasing drug concentrations over the study time.

To further understand the enhancement effect of the polymer on dissolution rate, the highest ranking ASD formulation (A, Lot 2), as shown in Figure 7, was selected for intrinsic dissolution studies. XRPD analysis of ASD disks produced by compression did not indicate devitrification of the samples. Figure 8 shows an initial 28-fold increase in intrinsic dissolution rate for the ASD sample compared to micronized AMG 517 crystalline material, and nearly a 2-fold initial increase compared with pure amorphous material. Results were based on determining the maximum slope of the dissolution curves for the crystalline and pure amorphous material, both of which were nonlinear beyond 15–25 min. In contrast, the load-corrected intrinsic dissolution rate (IDR) for the ASD formulation, measured to be  $0.32 \text{ mg/cm}^2\text{-min}$ , was constant over the 120 min experiment. The results indicate the ability of the hydrophilic polymeric carriers to significantly improve the *in vitro* dissolution, and thus possibly enhance the oral bioavailability of poorly soluble drugs. Dissolution rate in the ASD formulation was maintained at a higher relative rate throughout the experiment, whereas crystalline and pure amorphous rates diminished relatively rapidly.

Surfactants are well-known for the enhancement of wettability of drug products, and thus their frequent use in poorly soluble drug formulations. Poor wettability of ASD powders in aqueous medium was also observed from the various dissolution experiments. Poor wetting results in the ASD particles gelling into a mass rather than dispersing, slowing the dissolution rate. Therefore, to enhance the dissolution performance of ASD powders and powders in capsules, the effect of blending small quantities of a surfactant with the ASD powder was investigated in creating a prototype solid dosage form. Powder dissolution rate of micronized AMG 517 free base and ASD formulation A, Lot 2 (with and without 5 wt % sodium dodecyl sulfate) was carried out in

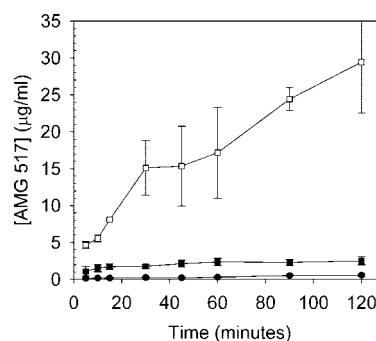


**Figure 9.** Powder dissolution profiles in 100 mL phosphate buffer, pH 6.8 (12.5 mg drug): (●) AMG 517 free base, micronized; (■) ASD formulation A, Lot 2 (15 wt % AMG 517 in HPMCAS) without SDS surfactant; (□) ASD formulation A, Lot 2 (15 wt % AMG 517 in HPMCAS) blended with 5 wt % SDS surfactant.

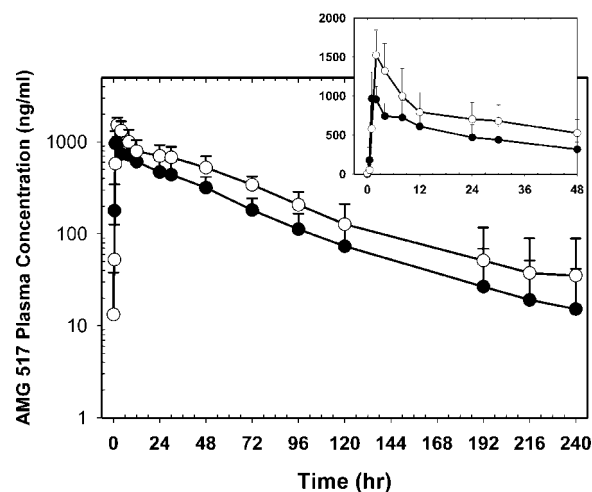


**Figure 10.** AMG 517 plasma concentration vs time profiles following oral administration at 12.5 mg AMG 517/animal to male cynomolgus monkeys ( $n = 6$ ) by (●) AMG 517 aqueous suspension in the 10% pluronic F108 Ora-Plus vehicle; (○) 15 wt % AMG 517 as an ASD in HPMCAS, blended with 5 wt % SDS and administered by capsule.

100 mL of pH 6.8 phosphate buffer as described. Overall resulting concentration of SDS in the dissolution medium was low ( $\sim 0.15 \text{ mM}$ ), well below the CMC of SDS ( $8.1 \text{ mM}$ ). As shown in Figure 9, the ASD powder with surfactant increased *in vitro* dissolution 12-fold over two hours, as compared to ASD powder without surfactant. Based on above studies, the 15 wt % AMG 517 in HPMCAS formulation (A, Lot 2,  $\sim 83 \text{ mg}$ ) coblended with 5 wt % SDS ( $\sim 4.2 \text{ mg}$ ) was selected as a prototype solid dosage form for PK evaluation.

**Pharmacokinetic Study.** An oral bioavailability study was conducted in fasted cynomolgus monkeys ( $n = 6$ , crossover) with the highest ranking ASD formulation from *in vitro* dissolution and the OraPlus suspension (as control reference). The mean plasma concentration–time profiles of AMG 517 are plotted against time in Figure 10. Plasma concentrations

**Table 2.** AMG 517 PK Parameters<sup>a</sup> and Summary Statistics Following Oral Administration at 12.5 mg/Animal to Male Cynomolgus Monkeys

formulation	$T_{\max}$ (h)	$C_{\max}$ (ng/mL)	AUC <sub>0–inf</sub> (ng h/mL)	$F_{\text{rel}}$ (%)
AMG 517 Ora-Plus suspension	1.5 (1.0–2.0)	1020 (189)	40800 (10300)	100
% CV	36.5	18.5	25.3	
AMG 517 ASD in capsule	2.0 (1.0–2.0)	1480 (309)	66600 (13200)	163
% CV	22.3	20.9	19.8	

<sup>a</sup>  $T_{\max}$ : Time at which  $C_{\max}$  was observed, presented as a median.  $C_{\max}$ : Maximum observed plasma concentration; AUC<sub>0–inf</sub> = Area under the plasma concentration–time curve from time zero to infinity.  $F_{\text{rel}}$  = bioavailability, relative to the suspension. The range of  $T_{\max}$  and standard deviation of other parameters are presented in parentheses.

of AMG 517 in Figure 10 are on the log scale and extended to 10 days; for clarity, the plasma concentrations in the inset plot are on a linear scale and extended to 48 h. The error bars observed at each point as determined from 6 monkeys were also shown in both plots. The PK parameters ( $C_{\max}$ ,  $T_{\max}$ , AUC, CV, etc.) of both formulations are summarized in Table 2.

Although both formulations showed rapid absorption with a short  $T_{\max}$  around 1–2 h, ASD formulation showed a significantly higher mean  $C_{\max}$  of 1480 ng/mL as compared to that (1020 ng/mL) of the OraPlus suspension (Table 2). Consistently, the area-under-the-curve (AUC) value of ASD formulation was approximately 163% of the OraPlus formulation, indicating a significant improvement in exposure. The variabilities of  $C_{\max}$  and AUC between the two formulations were comparable, as seen by the % CV in Table 2.

## Discussion

ASD powders of controlled size were prepared at low (15 wt %) and high (50 wt %) AMG 517 content by spray-drying HPMCAS and HPMC formulations with a laboratory-scale dryer. TGA weight loss of spray-dried particles indicated residual solvent levels of 2–3%, which was reduced by an additional vacuum drying operation. The film-forming tendency of HPMCAS and HPMC, enabling each to gel on removal of solvent, likely contributes to the observed corrugated morphology by SEM. It remains to be determined if the particles, as formed, would present considerable downstream challenges for efficient processing into a solid dosage form. Presently, the enlarged surface area of the particles and skinlike thickness of the polymer film could well have advantage in speeding the rate of swelling of the particles in use. In addition, removal of residual polymer solvent within the spray-drying process and secondary drying operation may likely be more efficient due to the shorter diffusional path lengths created by the corrugated structure.

ASD particles had a single  $T_g$  observed at 106 and 98 °C in HPMCAS matrices containing 15 wt % and 50 wt % AMG 517, respectively, and at 117 and 107 °C in HPMC-E5 matrices containing 15 wt % and 50 wt % AMG 517. The single  $T_g$  of the ASD matrices observed is significant, implying formation of solid dispersions; 15 wt % formulations did not devitrify on heating above the  $T_g$ . Actual glass transition temperature is dependent on the moisture content

of the sample, and hence the storage conditions.<sup>46,47</sup> During MDSC experiments, water (or solvent) loss from the sample is expected. The modulated DSC method employed resolves via the reversible heat-flow plots (Figure 3) the  $T_g$  transition from the nonreversible broad endothermic transition associated with moisture or solvent loss. The measured  $T_g$  value is thus likely greater than the  $T_g$  of the stored sample due to this loss of water or solvent during the DSC heating cycle. During method development, repeat scans through the  $T_g$  region did not show great variability in the measured  $T_g$ , suggesting most water or solvent was removed on first pass.  $T_g$  values thus presented are believed to be of samples devoid of most water and/or solvents. Secondary drying following spray-drying was an effective means for reducing moisture and solvent content of the ASD powders.

The  $T_g$  of a mixture ( $T_{g,\text{mix}}$ ) can be related to the  $T_g$  and mass fraction of the individual components within the mixture by the Gordon–Taylor/Kelly–Beuche relationship,<sup>48,49</sup> which assumes the two components are miscible and the free volumes of the components are additive. Assuming no specific interaction between the two components in the mixture:

$$T_{g,\text{mix}} = \frac{w_1 T_{g1} + K w_2 T_{g2}}{w_1 + K w_2} \quad (1)$$

where  $w_1$  and  $w_2$  represent the weight fractions for the two components,  $T_{g1}$  and  $T_{g2}$  are their respective glass transition temperatures, and  $K$  is the ratio of free volumes calculated using the relationship of Simha–Boyer:<sup>50</sup>

$$K = \frac{\rho_1 T_{g1}}{\rho_2 T_{g2}} \quad (2)$$

In eq 2,  $\rho_1$  and  $\rho_2$  are the respective densities of the amorphous materials.

- (46) Ford, J. L. Thermal analysis of hydroxypropylmethylcellulose and methylcellulose: powders, gels and matrix tablets. *Int. J. Pharm.* **1999**, 179 (2), 209–228.
- (47) Hancock, B. C.; Zografi, G. The relationship between the glass transition temperature and the water content of amorphous pharmaceutical solids. *Pharm. Res.* **1994**, 11 (4), 471–477.
- (48) Gordon, M.; Taylor, J. S. Ideal copolymers and the second-order transitions of synthetic rubbers 1: Non-crystalline copolymers. *J. Appl. Chem.* **1952**, 2, 493–498.
- (49) Kelley, F. N.; Bueche, F. Viscosity and glass temperature relations for polymer diluent systems. *J. Polym. Sci.* **1961**, 50, 549–556.
- (50) Simha, R.; Boyer, R. F. On a general relation involving the glass temperature and coefficients of expansion of polymers. *J. Chem. Phys.* **1962**, 37, 1003–1007.



The experimental  $T_g$  values can be compared with estimated values ( $T_{g,mix}$ ) according to the relationship in eq 1. The  $T_g$  of pure HPMCAS, HPMC-E5 and amorphous AMG 517 are approximately 119.5 °C, 154 °C,<sup>51</sup> and 103 °C, respectively. True density of HPMCAS is approximately 1.3 g/mL, as reported within the manufacture literature; true density of HPMC was reported as 1.19 g/mL.<sup>47</sup> True density of micronized AMG 517 (1.56 g/mL) was used as a surrogate for the true density of amorphous AMG 517. Varying the density value used in the Gordon–Taylor equation for AMG 517 by  $\pm 0.3$  g/mL did not change the outcome of our analysis significantly.

Experimental (Table 1) and theoretical (eq 1)  $T_{g,mix}$ 's deviated significantly, with the experimental values falling below those computed by the available parameters by 11 and 14 °C for HPMCAS at 15% and 50% drug load, and 20 and 29 °C for HPMC at 15% and 50% drug load. Within the literature, negative deviations from ideality have been observed when studying HPMC and HPMCAS.<sup>18,19</sup> The negative deviation from ideality suggests the free volume in the homogeneous phase is larger than in the ideal mixture, and relative weakness in the heteromolecular interactions within the solid.<sup>19</sup> As described above, the presence of residual solvent and moisture could also depress the determined  $T_g$  in these systems,<sup>7</sup> although for formulation A, Lot 2 the secondary dried material had a comparably low  $T_g$  as well. Formulations grouped by polymer trended toward lower  $T_g$  with increasing drug content, as expected by the theory, given the  $T_g$  of pure amorphous AMG 517 was less than the  $T_g$  of the polymers.

The physical stability evaluation of the HPMCAS ASD powders with a drug load of 15% and 50% indicated that AMG 517 remained at the amorphous state without detectable crystalline drug by XRPD at 40 °C/75% RH (open dish) for at least 6 months (evaluation limit). Hancock has asserted that molecular mobility becomes insignificant with respect to shelf life stability when amorphous materials are stored at 50 K below the  $T_g$ .<sup>27,31,52</sup> In the studied ASD formulations,  $T_g$ 's were all approximately 100 °C or greater, and would thus be expected to be storage stable at 40 °C. Maintaining the amorphous characteristics of the formulations for 6 months at elevated humidity indicates water uptake and  $T_g$  suppression in the AMG 517 amorphous system were not significant enough to impact physical stability. The presence of the polymer vastly improved storage stability under these conditions over the pure amorphous drug, suggesting the possibility of either an antiplasticization effect of the polymer under humid conditions or specific drug–carrier interaction

within the amorphous state of the dispersion.<sup>27,53</sup> Certainly, dispersing the drug in a carrier also contributed to improving storage stability.

Polymer type and concentration have been known to affect the dissolution rate and oral bioavailability of lipophilic drugs.<sup>54</sup> Although there was a clear trend with high and low drug load for each polymer, a polymer effect in the dissolution profile was not as apparent. ASD samples containing HPMCAS showed superior dissolution profile with higher supersaturation compared to HPMC-E5 at 15%, but the trend was reversed for 50%.

At low drug load (15%), enhanced dissolution rate for HPMCAS over HPMC-E5 may result from better wetting and water uptake of HPMCAS, on account of the higher number of hydrophilic carboxyl groups contained in the HPMCAS polymer. However, at higher drug loading (50%), the diminished dissolution profile for both polymers may not only be caused by the reduced polymer load, and therefore less water uptake, but may also be impacted by the reduced drug–polymer compatibility. Poorly compatible components, lacking specific drug–polymer interactions or miscibility, may phase demix at the surface of the solid dispersion during dissolution, potentially lowering dissolution rate. Observation of a constant intrinsic dissolution rate over 2 h for the lead ASD powder, 15% AMG 517 in HPMCAS-MF, suggests it had adequate drug–polymer compatibility; additional intrinsic dissolution data is required to assess the corresponding 50% ASD formulation for potential demixing.

Yu has recently proposed classifying compounds having intrinsic dissolution rates (IDRs) exceeding 0.1 mg/cm<sup>2</sup>/min as “high IDR” for purposes using IDR, rather than solubility, to classify drugs within the biopharmaceutics classification system (BCS).<sup>55,56</sup> Interestingly, the load-adjusted IDR obtained for the 15% AMG 517 in HPMCAS formulation, at 0.32 mg/cm<sup>2</sup>/min, effectively transitions AMG 517 from a “low IDR” compound as a crystal (0.011 mg/cm<sup>2</sup>/min) to a “high IDR” compound as an amorphous solid dispersion.

A comparative pharmacokinetic evaluation of the lead ASD formulation as a blend in a capsule (15 wt % AMG 517 in HPMCAS + 5% SDS) and an OraPlus suspension (as control reference) was conducted in cynomolgus monkeys ( $n = 6$ , crossover) at an AMG 517 dose of 12.5 mg. Such a dose was midrange of the 1–25 mg doses recently tested in humans.<sup>43</sup> PK results suggest that the ASD formulation

- (51) Joshi, H. N.; Wilson, T. D. Calorimetric studies of dissolution of hydroxypropyl methylcellulose E5 (HPMC E5) in water. *J. Pharm. Sci.* **1993**, 82 (10), 1033–8.
- (52) Hancock, B. C.; Shamblin, S. L.; Zografi, G. Molecular mobility of amorphous pharmaceutical solids below their glass transition temperatures. *Pharm. Res.* **1995**, 12 (6), 799–806.

- (53) Bhugra, C.; Pikal, M. J. Role of thermodynamic, molecular, and kinetic factors in crystallization from the amorphous state. *J. Pharm. Sci.* **2008**, 97 (4), 1329–49.
- (54) Dong, W.; Bodmeier, R. Encapsulation of lipophilic drugs within enteric microparticles by a novel coacervation method. *Int. J. Pharm.* **2006**, 326 (1–2), 128–138.
- (55) Amidon, G. L.; Lennernäs, H.; Shah, V. P.; Crison, J. R. A Theoretical Basis for a Biopharmaceutic Drug Classification: The Correlation of in Vitro Drug Product Dissolution and in Vivo Bioavailability. *Pharm. Res.* **1995**, 12 (3), 413–420.
- (56) Yu, L. X.; Carlin, A. S.; Amidon, G. L.; Hussain, A. S. Feasibility studies of utilizing disk intrinsic dissolution rate to classify drugs. *Int. J. Pharm.* **2004**, 270 (1–2), 221–227.

showed 163% of AUC, 145%  $C_{\max}$  and comparable  $T_{\max}$  ( $\sim 1-2$  h) as compared to the OraPlus formulation. It is worth emphasizing that OraPlus suspension was the best performer with the highest exposure and  $C_{\max}$  values in previous preclinical in vivo evaluations and a phase I clinical trial. The performance of the OraPlus suspension was attributed to formation of a more highly soluble cocrystal between AMG 517 and sorbic acid in the suspension.<sup>42</sup> However, the OraPlus suspension was not feasible for commercialization due to a low drug load ( $\sim 0.75$  mg/mL AMG 517) and large volume required for oral administration. Had the comparator in the monkey PK study been strictly micronized AMG 517 free base, the relative performance of the ASD formulation would have been even greater.

Collectively, in vitro dissolution and a comparative PK evaluation against an OraPlus suspension suggests rapid dissolution and a more complete absorption of AMG 517 via the amorphous solid dispersion approach. The ASD approach thus significantly improved oral bioavailability for a poorly soluble VR1 antagonist, while stabilizing the amorphous form of the molecule. Preparing ASD materials

at laboratory scale is a material-sparing operation which may be best applied at the discovery-development interface, in situations when low exposure is observed during high-dose toxicology evaluation due to a compound's poor solubility. In this setting, particle yield and quality of powders produced by spray-drying are adequate for rapidly evaluating the ASD approach.

### Abbreviations Used

ASD, amorphous solid dispersion; SD, spray-drying; SDS, sodium dodecyl sulfate; slpm, standard liters per minute; slph, standard liters per hour; XRPD, X-ray powder diffraction.

**Acknowledgment.** The authors wish to thank the following individuals for their support, input, and insight to this work: Karthik Nagapudi, Arun Koparkar, Glen Lawrence, Nina Cauchon, Paco Alvarez, Paul Burke, Peter Zhou, Mark Rose, Fernando Alvarez-Nunez, Anu Gore and Kirby Wong-Moon. Thanks also to Tom Menges for arranging the PK study.

MP800061R